Electrically-controlled Nonlinear Magnon-Magnon Coupling in Synthetic Antiferromagnet

A. Sud,[1,2] K. Yamamoto,[3] S. Iihama,[1,4] K. Ishibashi,[5,4] S. Fukami,[2,4,6] H. Kurebayashi,[7,8,4] and S. Mizukami[4,6,*]

[1] *Frontier Research Institute for Interdisciplinary Sciences, Tohoku University, 6-3 Aoba, Sendai 980-8578, Japan*
[2] *Research Institute of Electrical Communication, Tohoku University, 2-1-1 Katahira, Sendai, 980-8577, Japan*
[3] *Advanced Science Research Center, Japan Atomic Energy Agency, 2-4 Shirakata, Tokai 319-1195, Japan*
[4] *WPI Advanced Institute for Materials Research, Tohoku University, 2-1-1 Katahira, Sendai 980-8577, Japan*
[5] *Department of Applied Physics, Tohoku University, 6-6-05 Aoba, Sendai 980-8579, Japan.*
[6] *Center for Science and Innovation in Spintronics, Tohoku University, 2-1-1 Katahira, Sendai 980-8577 Japan*
[7] *London Centre for Nanotechnology, University College London, 17-19 Gordon Street, London, WC1H 0AH, United Kingdom*
[8] *Department of Electronic and Electrical Engineering, University College London, London, WC1E 7JE, United Kingdom*

(Dated: May 16, 2025)

We investigate the nonlinear coupling between acoustic (ac) and optical (op) modes in the coupled magnetization dynamics of synthetic antiferromagnets (SyAFs), utilizing current-driven resonance spectroscopy. A clear spectral splitting is evident in the ac mode when strongly excited by the radio frequency (RF) current at the driving frequency half that of the op mode resonance. The Landau-Lifshitz phenomenology aligns with the experimental observations, affirming the coupling of the RF-excited ac and op modes through three-magnon mixing. The nonlinearity enables a Rabi-like splitting in in-plane magnetized SyAF without breaking its natural symmetries. This discovery holds potential for advancing our understanding of nonlinear antiferromagnetic dynamics.

The coupling between two harmonic oscillators has garnered considerable attention and has been extensively investigated in classical [1] and quantum systems [2, 3], as well as in hybrid systems [4, 5]. In quantum mechanics, when two degenerate resonators with the mode frequency ω_0 undergo mode coupling, they exhibit two resonance frequencies $\omega = \omega_0 \pm \delta\omega$. The resultant mode splitting, $2\delta\omega$, is referred to as the Rabi splitting in quantum physics. This phenomenon has been thoroughly discussed from both classical and quantum mechanical perspectives [6, 7] till date. In particular, strong coupling involving magnons has attracted recent interest for coherent manipulation of spin degrees of freedom [8–18].

Significant research is also underway to explore the coupling physics in synthetic antiferromagnets (SyAFs) [Fig. 1(a)]. In SyAF structures, two magnetic layers are separated by a thin non-magnetic spacer, with their magnetizations antiferromagnetically coupled via electronic spin polarization within the spacer layer. In the context of antiferromagnetic spintronics [19, 20], it makes them an attractive alternative to elemental antiferromagnets for their tunability and amenability to well-established ferromagnetic resonance techniques [21, 22]. The system possesses two spatially uniform magnon eigenmodes: the in-phase (acoustic (ac)) mode resembling ferromagnetic behavior and the out-of-phase (optical (op)) mode with characteristically antiferromagnetic properties. Additionally, magnons in SyAFs propagating in-plane and perpendicular to the magnetization of the magnetic layers exhibit nonreciprocal dispersion, as detailed in recent studies ([23, 24]). The resonance frequencies $\omega_{\rm ac}$, $\omega_{\rm op}$ of the respective modes can be widely tuned by adjusting the strength and direction of an externally applied static magnetic field H. While there exists a field range where $\omega_{\rm ac} \sim \omega_{\rm op}$, the resonance spectrum does not necessarily show the anti-crossing behavior characteristic of coupling of the two modes. In the linear regime, it requires breaking of a symmetry $\mathcal{S}$ (two-fold rotation about the field direction followed by interchange of the two magnetic layers), by either exciting obliquely propagating waves [25], tilting the field out-of-plane [26, 27], or using inequivalent top and bottom magnetic layers [28, 29].

Here, we pursue an alternative path to achieve the coupling of ac and op magnon modes [Fig. 1(b)] without breaking the symmetry $\mathcal{S}$, by exploiting nonlinearity of magnon dynamics. For H directed in the plane and under certain modelling assumptions, one may readily derive from the perturbative expansion of Landau-Lifshitz equations for SyAF (see Supplemental Material (SM) [30] for details of derivation)

$$i\frac{db_{\rm ac}}{dt} = (\omega_{\rm ac} - i\kappa_{\rm ac})\, b_{\rm ac} + 2ig_3 b_{\rm ac}^* b_{\rm op} + \tau_{\rm ac}, \qquad (1)$$

$$i\frac{db_{\rm op}}{dt} = (\omega_{\rm op} - i\kappa_{\rm op})\, b_{\rm op} - ig_3 b_{\rm ac}^2 + \tau_{\rm op}, \qquad (2)$$

where $b_{\rm ac}, b_{\rm op}$ are the complex amplitudes of ac and op magnon eigenmodes, $\kappa_{\rm ac(op)}$, and $\tau_{\rm ac(op)}$ denote the

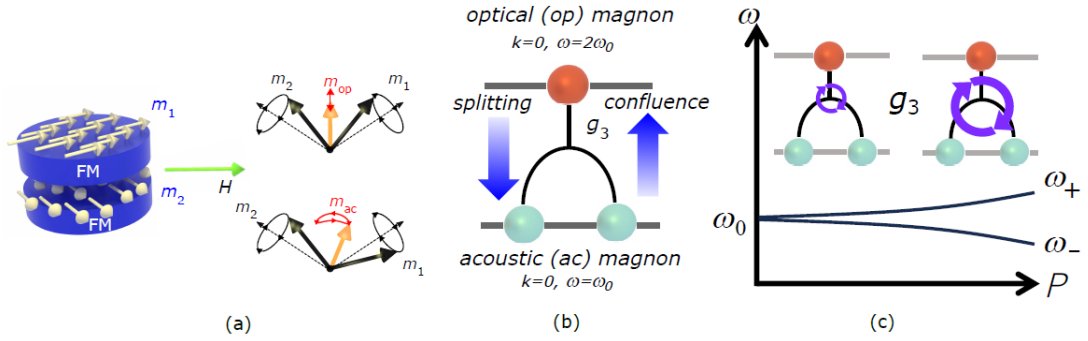

FIG. 1. (a) Schematic illustration of synthetic antiferromagnet (SyAF) sample consisting of two ferromagnetic (FM) layers. The magnetizations m_1 and m_2 are canted upon application of an external magnetic field H. (b) Schematic of the three-magnon confluence and splitting processes between ac (ω_0) and op ($2\omega_0$) magnons with three-magnon mixing g_3. When the input excitation power P becomes very large, the ac magnon spectrum exhibits two peaks $\omega_{+(-)}$ due to the nonlinear coupling as shown in (c).

damping rate and external radio-frequency (RF) torque for the ac (op) mode, and the coefficient g_3 represents three-magnon mixing. The three-magnon mixing processes include frequency down-conversion (splitting) and up-conversion (confluence), as depicted in Fig. 1(b), and have been experimentally studied using both low-damping magnetic insulators and metallic ferromagnets [31–36]. Throughout the article, the magnon modes $b_{\rm ac}, b_{\rm op}$ refer to spatially uniform modes. All the terms contained in Eqs. (1) and (2) describe the ac and op magnon modes, in particular $b_{\rm ac}^* b_{\rm op}$ and $b_{\rm ac}^2$, transform under the odd and even irreducible representations of $\mathcal{S}$ respectively. One observes that $ig_3 b_{\rm ac}$ acts like a linear coupling between $b_{\rm ac}$ and $b_{\rm op}$ and can anticipate a Rabi-like splitting in the spectrum when $b_{\rm ac}$ acquires a sufficient amplitude such that $|g_3 b_{\rm ac}| \gtrsim \kappa_{\rm ac}, \kappa_{\rm op}$ [Fig. 1(c)]. While the equations are formally identical to those studied in the nonlinear cavity photonics and opto-mechanics [37–43], SyAF magnons offer advantages over photons in their tunability and the large coupling g_3 that turns out to be of order $\omega_{\rm ac}$, $\omega_{\rm op}$ when $|b_{\rm ac}|^2$ is normalized to represent the number of excited ac magnons per spin. Nonlinear antiferromagnetic dynamics has been a subject of fundamental importance, although its progress has been hindered, partially due to the lack of materials with accessible resonance characteristics [44–46]. In this letter, we aim at advancing the understanding of antiferromagnetic nonlinearity by leveraging the unique properties of SyAF magnons. We experimentally proved the presence of the nonlinear frequency splitting in SyAF. Using state-of-the-art spectroscopic techniques, we measured the response of SyAF under various conditions to identify the signatures of nonlinear frequency splitting. By analyzing the frequency spectra, we were able to observe clear evidence of nonlinear interactions that had not been previously documented in SyAF. The present finding demonstrates SyAF as a promising platform for exploring nonlinear mode coupling phenomena.

We employed the previously established excitation and detection scheme for ac and op magnon dynamics in SyAF, as illustrated in Fig. 2(a) (see the details in Ref. [47]). The SyAF sample utilized in this study comprised of Si/SiO_2/Ta(5)/NiFe(5)/Ru(0.5)/NiFe(5)/Ta(5) layers (with thicknesses specified in nm), fabricated via ultra-high vacuum magnetron sputtering. An amplitude modulated RF current was applied to the SyAF through a coplanar waveguide and RF probe [Fig. 2(a)]. Magnetization dynamics was excited by field-like and damping-like torques induced by the RF current and detected as a rectified voltage using a lock-in amplifier under an in-plane magnetic field. Note that the present setup probes only modes spatially uniform in the in-plane directions while perpendicular standing spin waves are of much higher frequencies than several GHz for such small film thicknesses.

In the absence of field H, the SyAF demonstrates collinear, anti-parallel and in-plane magnetizations due to the interlayer antiferromagnetic exchange coupling represented by the exchange field, $H_{\rm ex}$. Upon the application of an in-plane magnetic field ($H < 2H_{\rm ex}$), these magnetizations become canted, as depicted in Fig. 1(a), with the two magnon mode resonance frequencies expressed as: $\omega_{\rm ac} = \gamma\mu_0 H\sqrt{1+\frac{M_{\rm s}}{2H_{\rm ex}}}$ and $\omega_{\rm op} = 2\gamma\mu_0 H_{\rm ex}\sqrt{\frac{M_{\rm s}}{2H_{\rm ex}}\left(1-\frac{H^2}{4H_{\rm ex}^2}\right)}$, where γ, μ_0, and $M_{\rm s}$ represents the gyromagnetic ratio, vacuum permeability, and the saturation magnetization of the ferromagnetic layer, respectively. As H increases, $\omega_{\rm ac}$ linearly rises, while $\omega_{\rm op}$ gradually decreases. This progression leads to the fulfillment of double resonance condition $2\omega_{\rm ac} = \omega_{\rm op}$ at a specific magnetic field strength, $H_{\rm c} = 2H_{\rm ex}/\sqrt{5+8H_{\rm ex}/M_{\rm s}}$, as illustrated in Fig. 2(b). Figures 2(c) and 2(d) depict the RF spectra observed experimentally under various

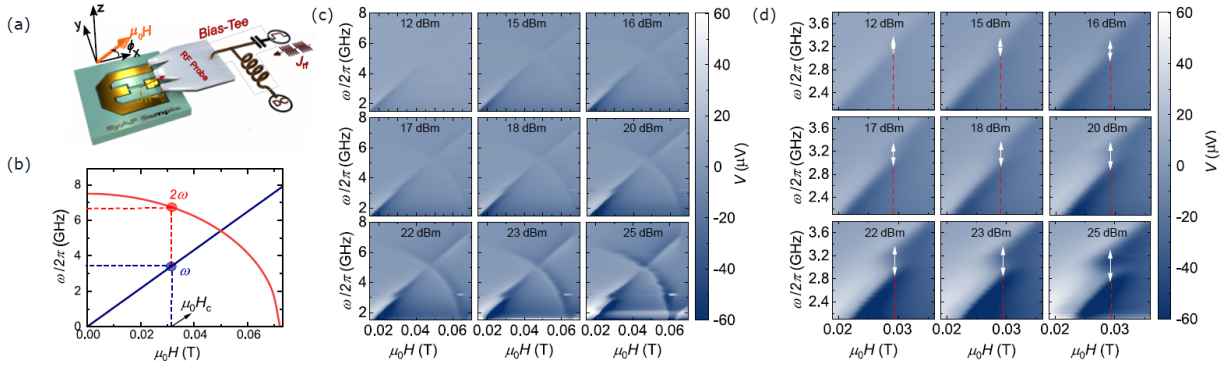

FIG. 2. Experimental setup used for the measurements. A microwave RF current $J_{\rm rf}$ at frequency ω and power P is injected into the bar with width 10 μm through a bias-tee and RF probe. Here, ϕ denotes the angle between the direction of injected current and the applied field, $\mu_0 H$. The rectified voltage signal V is then detected via lock-in amplifier. In linear regime the frequencies for ac and op mode show different H dependence as indicated in (b). At double resonance condition $2\omega_{\rm ac} = \omega_{\rm op}$, which occurs at field denoted by $H_{\rm c}$, a gap is seen in the ac mode spectra. (c) shows the rectified voltages obtained as a function of field and frequency for different input power, P at $\phi = 45°$. A splitting is seen in the ac mode spectra around 3 GHz which is more apparent at higher P. (d) shows the zoom-in version of (c). The arrows in (d) indicate the splitting at $H_{\rm c}$ (indicated by red vertical lines).

magnetic field strengths and incident power, P. The ac and op magnon resonances are identified with the contrast changes along the nearly straight lines and almost a quarter circle, respectively. We specifically selected a magnetic field angle of 45° with respect to the current direction to ensure the excitation and detection of both modes [47]. At lower power levels, approximately below 12 dBm, linear dynamics is observed, as shown in the top panels of Figs. 2(c) and 2(d). In contrast, when the power exceeds approximately 12 dBm, the ac mode begins to exhibit splitting at $H = H_{\rm c}$. This splitting becomes increasingly pronounced with higher power levels, as demonstrated in the bottom panels of Figs. 2(c) and 2(d).

For a more quantitative analysis, we determine the splitting and other relevant parameters by fitting the experimental data using the symmetric and anti-symmetric Lorentzian function(s)as detailed in SM [30]. Figures 3(a) and 3(b) show the power dependence of the extracted resonance frequencies for the ac and op modes and the gap observed in the ac mode spectrum respectively. These values were obtained at $H_{\rm c}$ of around 29.0 mT, where $H_{\rm c}$ slightly increases with increasing P, up to 29.5 mT [30], likely due to Joule heating. As illustrated in Fig. 3(b), the observed gap $(\omega_+ - \omega_-)/2\pi$ reaches 0.45 GHz where, $\omega_+(\omega_-)$ is the frequency of upper (lower) branch split from the ac mode as shown in Fig. 3(a). The gap observed at high P is larger than the ac mode damping rate $\kappa_{\rm ac}/2\pi$ of 0.225 GHz, and comparable to that of the op mode damping rate $\kappa_{\rm op}/2\pi$ of 0.470 GHz evaluated from the frequency-dependent linewidth of the field-swept FMR at $P = 4$ dBm, low enough to neglect the nonlinear effects (see SM [30]). The observed gap exceeds the relaxation rate of the acoustic mode and approaches that of the optical mode, indicating that the system is approaching the so-called strong coupling regime. Let us now identify the origin of the gap from theoretical perspectives. To facilitate the interpretation of the spectral gap using Eqs. (1) and (2), we restrict our attention mainly to the double resonance condition $2\omega_{\rm ac} = \omega_{\rm op}$. Substituting the ansatz $b_{\rm ac} = c_{\rm ac} e^{-i\omega t}, b_{\rm op} = c_{\rm op} e^{-2i\omega t}, \tau_{\rm ac} = \tilde{\tau} e^{-i\omega t}, \tau_{\rm op} = 0$ with constant $c_{\rm ac}, c_{\rm op}, \tilde{\tau}$ and excitation frequency ω yields

$$\begin{pmatrix} \omega - \omega_{\rm ac} + i\kappa_{\rm ac} & G^* \\ G & \omega - \omega_{\rm ac} + i\frac{\kappa_{\rm op}}{2} \end{pmatrix} \begin{pmatrix} c_{\rm ac} \\ 2c_{\rm op} \end{pmatrix} = \begin{pmatrix} \tilde{\tau} \\ 0 \end{pmatrix}, \quad (3)$$

where $G = ig_3 c_{\rm ac}$. Note that G depends on ω through $c_{\rm ac}$ so that this is not a linear eigenvalue problem. For the time being, however, we proceed as if G were a constant. Setting the left-hand-sides zero yields

$$\omega = \omega_{\rm ac} - \frac{i}{2}\left\{\kappa_{\rm ac} + \frac{\kappa_{\rm op}}{2} \pm \sqrt{\left(\kappa_{\rm ac} - \frac{\kappa_{\rm op}}{2}\right)^2 - 4|G|^2}\right\}. \quad (4)$$

The splitting of ac mode occurs when the condition $\left(\kappa_{\rm ac} - \frac{\kappa_{\rm op}}{2}\right)^2 - 4|G|^2 < 0$ is satisfied, namely at the exceptional point within the realm of non-Hermitian physics [48, 49]. This condition can also be written as $|b_{\rm ac}| > \left|\kappa_{\rm ac} - \frac{\kappa_{\rm op}}{2}\right| / |g_3|$, which can be compared with the threshold for three-magnon instability $|b_{\rm op}| > \kappa_{\rm ac}/|g_3|$ [50]. The comparison highlights not only the similarly small amplitudes of magnons required to observe the respective phenomena, but also the fundamental difference between them in that the conditions refer to different magnon modes. As explained in the context of photonics [37], the conventional threshold refers to the onset of parametric instability while what we pursue here is a second harmonic generation that has no threshold.

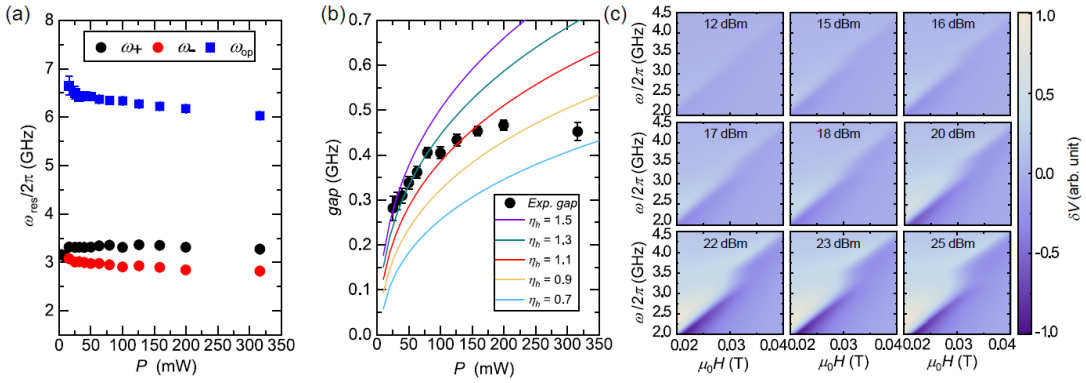

FIG. 3. (a) The resonance frequency for the ac and op modes obtained from the FMR spectrum in frequency domain at $H = H_c$ via least-square fitting of Lorentz curves. The splitting in ac mode occurs near 3.0 GHz and shows upper ω_+ and lower ω_- branches. (b) Gap in the ac mode spectra as a function of input power P, obtained from the difference of ω_+ and ω_- . Curves are theoretically obtained values with different η_h. Note that we plot the data with linear scales for horizonal axes in (a) and (b). (c) The theoretical simulation of the voltage for an η_h of 1.3 as a function of frequency and field with different microwave input powers.

Its observation via nonlinear spectral splitting, however, requires sufficiently large $|b_{ac}|$, which happens to be virtualy zero in our sample due to $\kappa_{ac} \sim \kappa_{op}/2$. For b_{ac} normalized such that $|b_{ac}|^2$ equals the number of ac magnons excited per microscopic spin site, the three-magnon coefficient is given by [30]

$$g_3 = \frac{\gamma\mu_0 H}{8}\sqrt{1-\frac{H^2}{4H_{ex}^2}}\sqrt{\frac{\gamma\mu_0 M_s}{\omega_{op}}} \times \left(\frac{2\omega_{op}}{\gamma\mu_0 M_s}+\frac{\gamma\mu_0 H^2}{2H_{ex}\omega_{ac}}+\frac{2H_{ex}\omega_{ac}}{\gamma\mu_0 H^2}\right). \quad (5)$$

While H_{ex} varies with the RF current J_{rf}, $g_3/2\pi \approx 1.5$ GHz depends only weakly on H_{ex} across the experimental conditions. This implies we start seeing the gap when $|c_{ac}| \gtrsim 0.1$, which means only a magnon per 100 spin sites is excited and the perturbative picture is justifiable.

For further understanding, we conducted numerical simulations, using the parameters determined through a mulitple step fitting procedure detailed in SM [30]. As already discussed, $|G|$ is proportional to the ac mode amplitude $|c_{ac}|$ which in the linear response regime is proportional to J_{rf} applied to the sample; that is, $|G| \sim g_3 |c_{ac}| \propto \sqrt{P}$. However, this relationship does not hold true in our current study. In the nonlinear regime of our investigation, $|c_{ac}|^2$ at $H = H_c$ is determined by solving Eq. (3) for c_{ac}, which yields the following third-order algebraic equation:

$$\left[\left(g_3^2|c_{ac}|^2+\frac{\kappa_{ac}\kappa_{op}}{2}\right)^2+\left\{g_3^2|c_{ac}|^2+\left(\kappa_{ac}-\frac{\kappa_{op}}{2}\right)^2\right\}(\omega-\omega_{ac})^2+(\omega-\omega_{ac})^4\right]|c_{ac}|^2 = \left\{(\omega-\omega_{ac})^2+\frac{\kappa_{op}^2}{4}\right\}|\tilde{\tau}|^2. \quad (6)$$

This expression indicates that the amplitude of the ac mode exhibits linear behavior in the external torque $\tilde{\tau}$ only when the condition $|c_{ac}| \ll \kappa_{ac}\kappa_{op}/2g_3^2$ is met. By taking account of the current-induced Oersted field as well as the damping-like spin-orbit torque [30], $\tilde{\tau}$ can be written as

$$\tilde{\tau} = -\gamma\mu_0\sqrt{1-\frac{H^2}{4H_{ex}^2}}\frac{J_{rf}}{4w}\sqrt{\frac{\gamma\mu_0 H^2}{H_{ex}\omega_{ac}}} \times \left(\frac{\eta_j\hbar\theta_{SH}}{e\mu_0 M_s d_{FM} d_{Ta}}-i\frac{2\eta_h H_{ex}\omega_{ac}}{\gamma\mu_0 H^2}\right), \quad (7)$$

where θ_{SH} is the spin-Hall angle, $\hbar$ is the reduced Planck's constant, e is the elementary charge and w, d_{FM}, d_{Ta} are the width of the bar and thickness of the ferromagnetic and heavy metal layer respectively. The dimensionless parameters η_j, η_h depend on the current distribution across the film stack and are taken as effective fitting parameters that also account for other possible mechanisms of the damping-like and field-like rf torque contributions. A simple model for the current distribution is given in SM [30] to demonstrate that η_j, η_h are typically of order unity.

We solved Eq. (6), and then Eq. (3) for $H = H_c$ to obtain c_{ac} as a function of f and P_{in}. The theoretical estimate for the gap was obtained by fitting $\delta V \propto \Im[c_{ac}] J_{rf}$ with the same double Lorentzian function as in the ex-

perimental data analysis, which is presented in Fig. 3(b). We used the parameters of $\gamma/2\pi = 29.5$ GHz/T, $M_s = 720$ kA/m, and $\mu_0 H_{ex} = 36.2$ mT extracted from the field-swept FMR data at 4 dBm that also shows that the anti-symmetric Lorentzian component dominates over the symmetric one [30] and justifies setting $\eta_j \theta_{SH} = 0$ for simplicity [51], leaving η_h as the only free parameter in the model. For quantitative comparison, we calibrated J_{rf} as a function of P_{in} by the bolometric method [30]. The order of magnitude of the observed gap is consistent with $\eta_h \sim 1$, while the experimental gap saturates more quickly. This type of discrepancy is expected as the perturbative study is meant to capture only the onset of nonlinear effects. The observed power dependence of resonance frequencies and linewidths appears too weak to cause the saturation which also occurs away from the double resonance as presented in SM [30], leaving its origin an open question. Figure 3(c) illustrates the example of variation of the ac magnon mode spectrum computed with different powers, in which we used $\eta_h = 1.3$ that fits the experimental gap well in the low power regime in Fig. 3(b). It reproduces the splitting at $H_c \sim 30$ mT with increasing J_{rf} as observed in the experiment. The result validates the interpretation of the ac mode spectral splitting in terms of nonlinear magnon-magnon coupling via three-magnon mixing. Note that $\eta_h \gtrsim 1$ indicates an additional source of field-like torque other than the Oersted field, whereas more quantitative modeling is beyond the scope of this Letter not least because of the lack of direct access to the experimental rf current distribution.

We stress that we have observed a clear Rabi-like splitting arising from nonlinear magnon-magnon coupling despite the relatively large damping κ_{ac}/ω_{ac} of roughly 10%. This is in contrast to the strong coupling observed in cavity-photonics devices, where ultra-low loss cavities with a quality factor, Q of about $10^5 - 10^6$ were employed [40, 41]. It is down to the common origin of linear and nonlinear terms in the magnon Hamiltonian for SyAF, both governed by H_{ex} and M_s. Combined with the ample room for parameter tuning and optimization, our findings suggest SyAF as a promising platform for exploring broader range of nonlinear phenomena. g_3 corresponds to $\chi^{(2)}$ nonlinearity in photonics, which was generated effectively through a higher-order nonlinearity [40, 41]. Upon increasing the amplitude beyond the Rabi-like splitting, $\chi^{(2)}$ is known to cause instability of the second harmonic fixed point studied in the present work that evolves into a self-pulsing behavior [52–55]. The onset of the transition is characterized by the critical value [37], $|G_{th}| = \sqrt{\frac{\kappa_{ac}(\kappa_{ac}+\kappa_{op})}{2}}$. The sample employed in the present study does not quite reach but is tantalizingly close to this point. Lower damping rates κ_{ac} and κ_{op}, along with higher three-magnon mixing coefficient g_3, are achievable by carefully selecting ferromagnetic and non-magnetic materials and optimizing stacking structures. While the present study provides the first evidence of nonlinear strong coupling in SyAFs, yet unexplored dynamics may emerge from nonlinear magnon-magnon interactions, and potentially be extended to quantum magnon physics through cryogenic experiments.

In summary, we realized the strong coupling regime of ac and op magnon modes in SyAF by a second-order nonlinear coupling between them, specifically, through coherent three-magnon processes. By directly injecting RF current into SyAF, we generated sufficiently large amplitudes of ac magnons, enabling us to achieve a Rabi-like spectral splitting despite the presence of sizeable damping rates. The experimental results closely match our theoretical model which thoroughly accounts for three-magnon mixing, supporting our interpretation. The present findings open an array of possibilities in advancing our understanding of nonlinear dynamical phenomena through material choices and structural optimization of SyAF.

A. S. thanks JSPS Postdoctoral fellowship for research in Japan (P21777). K. Y. is supported by JST PRESTO Grant No. JPMJPR20LB, Japan, JSPS KAKENHI (No. 21K13886, 24K00576), and JSPS Bilateral Program Number JPJSBP120245708. S. M. thanks to CSRN in CSIS at Tohoku Univ. and to JSPS KAKENHI (No. 21H04648, 21H05000, 22F21777, 22KF0030) and X-NICS of MEXT (No. JPJ011438). K. I. thanks to GP-SPIN at Tohoku Univ. H. K. acknowledges Engineering and Physical Sciences Research Council for support via grant EP/X015661/1, and UCL for UCL-Tohoku University Strategic Partner Fund. S. F. thanks to JSPS KAKENHI (No. 24H00039, 24H02235).

* shigemi.mizukami.a7@tohoku.ac.jp

[1] L. Novotny, Strong coupling, energy splitting, and level crossings: A classical perspective, American Journal of Physics **78**, 1199 (2010).
[2] B. Mollow, Quantum statistics of coupled oscillator systems, Physical Review **162**, 1256 (1967).
[3] R. Graham and M. Höhnerbach, Quantum chaos of the two-level atom, Physics Letters A **101**, 61 (1984).
[4] R. J. Glauber, Classical behavior of systems of quantum oscillators, Physics Letters **21**, 650 (1966).
[5] S. R.-K. Rodriguez, Classical and quantum distinctions between weak and strong coupling, European Journal of Physics **37**, 025802 (2016).
[6] G. Agarwal, Vacuum-field Rabi splittings in microwave absorption by Rydberg atoms in a cavity, Physical Review Letters **53**, 1732 (1984).
[7] J. Sanchez-Mondragon, N. Narozhny, and J. Eberly, Theory of spontaneous-emission line shape in an ideal cavity, Physical Review Letters **51**, 550 (1983).
[8] B. Zare Rameshti, S. Viola Kusminskiy, J. A. Haigh, K. Usami, D. Lachance-Quirion, Y. Nakamura, C.-M. Hu, H. X. Tang, G. E. Bauer, and Y. M. Blanter, Cavity

magnonics, Physics Reports **979**, 1 (2022).
[9] D. D. Awschalom, C. R. Du, R. He, F. J. Heremans, A. Hoffmann, J. Hou, H. Kurebayashi, Y. Li, L. Liu, V. Novosad, J. Sklenar, S. E. Sullivan, D. Sun, H. Tang, V. Tyberkevych, C. Trevillian, A. W. Tsen, L. R. Weiss, W. Zhang, X. Zhang, L. Zhao, and C. W. Zollitsch, Quantum engineering with hybrid magnonic systems and materials (invited paper), IEEE Transactions on Quantum Engineering **2**, 1 (2021).
[10] X. Zhang, C.-L. Zou, L. Jiang, and H. X. Tang, Strongly coupled magnons and cavity microwave photons, Physical Review Letters **113**, 156401 (2014).
[11] Y. Tabuchi, S. Ishino, A. Noguchi, T. Ishikawa, R. Yamazaki, K. Usami, and Y. Nakamura, Coherent coupling between a ferromagnetic magnon and a superconducting qubit, Science **349**, 405 (2014).
[12] L. Bai, M. Harder, Y. P. Chen, X. Fan, J. Q. Xiao, and C.-M. Hu, Spin pumping in electrodynamically coupled magnon-photon systems, Physical Review Letters **114**, 227201 (2015).
[13] S. Klingler, V. Amin, S. Geprägs, K. Ganzhorn, H. Maier-Flaig, M. Althammer, H. Huebl, R. Gross, R. D. McMichael, M. D. Stiles, S. T. B. Goennenwein, and M. Weiler, Spin-torque excitation of perpendicular standing spin waves in coupled YIG/Co heterostructures, Physical Review Letters **120**, 127201 (2018).
[14] J. Chen, C. Liu, T. Liu, Y. Xiao, K. Xia, G. E. W. Bauer, M. Wu, and H. Yu, Strong interlayer magnon-magnon coupling in magnetic metal-insulator hybrid nanostructures, Physical Review Letters **120**, 217202 (2018).
[15] Y. Li, T. Polakovic, Y.-L. Wang, J. Xu, S. Lendinez, Z. Zhang, J. Ding, T. Khaire, H. Saglam, R. Divan, et al., Strong coupling between magnons and microwave photons in on-chip ferromagnet-superconductor thin-film devices, Physical Review Letters **123**, 107701 (2019).
[16] D. MacNeill, J. T. Hou, D. R. Klein, P. Zhang, P. Jarillo-Herrero, and L. Liu, Gigahertz frequency antiferromagnetic resonance and strong magnon-magnon coupling in the layered crystal $CrCl_3$, Physical Review Letters **123**, 047204 (2019).
[17] S. Liu, A. G. Del Águila, D. Bhowmick, C. K. Gan, T. T. H. Do, M. Prosnikov, D. Sedmidubskỳ, Z. Sofer, P. C. Christianen, P. Sengupta, et al., Direct observation of magnon-phonon strong coupling in two-dimensional antiferromagnet at high magnetic fields, Physical Review Letters **127**, 097401 (2021).
[18] J. Rao, C. Wang, B. Yao, Z. Chen, K. Zhao, and W. Lu, Meterscale strong coupling between magnons and photons, Physical Review Letters **131**, 106702 (2023).
[19] T. Jungwirth, X. Marti, P. Wadley, and J. Wunderlich, Antiferromagnetic spintronics, Nature Nanotechnology **11**, 231 (2016).
[20] S. Fukami, V. O. Lorenz, and O. Gomonay, Antiferromagnetic spintronics, Journal of Applied Physics **128**, 070401 (2020).
[21] J. Lindner and K. Baberschke, In situ ferromagnetic resonance: an ultimate tool to investigate the coupling in ultrathin magnetic films, Journal of Physics: Condensed Matter **15**, R193 (2003).
[22] M. Farle, Ferromagnetic resonance of ultrathin metallic layers, Reports on Progress in Physics **61**, 755 (1998).
[23] R. Gallardo, T. Schneider, A. Chaurasiya, A. Oelschlägel, S. Arekapudi, A. Roldán-Molina, R. Hübner, K. Lenz, A. Barman, J. Fassbender, et al., Reconfigurable spin-wave nonreciprocity induced by dipolar interaction in a coupled ferromagnetic bilayer, Physical Review Applied **12**, 034012 (2019).
[24] F. Millo, J.-P. Adam, C. Chappert, J.-V. Kim, A. Mouhoub, A. Solignac, and T. Devolder, Unidirectionality of spin waves in synthetic antiferromagnets, Physical Review Applied **20**, 054051 (2023).
[25] Y. Shiota, T. Taniguchi, M. Ishibashi, T. Moriyama, and T. Ono, Tunable magnon-magnon coupling mediated by dynamic dipolar interaction in synthetic antiferromagnets, Physical Review Letters **125**, 017203 (2020).
[26] A. Sud, C. Zollitsch, A. Kamimaki, T. Dion, S. Khan, S. Iihama, S. Mizukami, and H. Kurebayashi, Tunable magnon-magnon coupling in synthetic antiferromagnets, Physical Review B **102**, 100403 (2020).
[27] C. Dai and F. Ma, Strong magnon–magnon coupling in synthetic antiferromagnets, Applied Physics Letters **118** (2021).
[28] M. Li, J. Lu, and W. He, Symmetry breaking induced magnon-magnon coupling in synthetic antiferromagnets, Physical Review B **103**, 064429 (2021).
[29] A. Sud, K. Yamamoto, K. Suzuki, S. Mizukami, and H. Kurebayashi, Magnon-magnon coupling in synthetic ferrimagnets, Physical Review B **108**, 104407 (2023).
[30] See Supplemental Material at URL-will-be-inserted-by-publisher for additional information of the perturbative expansion and model of Second Harmonic Generation.
[31] P. Wigen, R. McMichael, and C. Jayaprakash, Route to chaos in the magnetic garnets, Journal of Magnetism and Magnetic Materials **84**, 237 (1990).
[32] C. Mathieu, V. T. Synogatch, and C. E. Patton, Brillouin light scattering analysis of three-magnon splitting processes in yttrium iron garnet films, Physical Review B **67**, 104402 (2003).
[33] H. Kurebayashi, O. Dzyapko, V. E. Demidov, D. Fang, A. J. Ferguson, and S. O. Demokritov, Controlled enhancement of spin-current emission by three-magnon splitting, Nature Materials **10**, 660 (2011).
[34] L. Körber, K. Schultheiss, T. Hula, R. Verba, J. Faßbender, A. Kákay, and H. Schultheiss, Nonlocal stimulation of three-magnon splitting in a magnetic vortex, Physical Review Letters **125**, 207203 (2020).
[35] I. Barsukov, H. Lee, A. Jara, Y.-J. Chen, A. Gonçalves, C. Sha, J. Katine, R. Arias, B. Ivanov, and I. Krivorotov, Giant nonlinear damping in nanoscale ferromagnets, Science Advances **5**, eaav6943 (2019).
[36] T. Qu, A. Hamill, R. Victora, and P. Crowell, Oscillations and confluence in three-magnon scattering of ferromagnetic resonance, Physical Review B **107**, L060401 (2023).
[37] P. Drummond, K. McNeil, and D. Walls, Non-equilibrium transitions in sub/second harmonic generation, Optica Acta: International Journal of Optics **27**, 321 (1980).
[38] I. Carusotto and G. C. La Rocca, Two-photon rabi splitting and optical stark effect in semiconductor microcavities, Physical Review B **60**, 4907 (1999).
[39] W. T. Irvine, K. Hennessy, and D. Bouwmeester, Strong coupling between single photons in semiconductor microcavities, Physical Review Letters **96**, 057405 (2006).
[40] X. Guo, C.-L. Zou, H. Jung, and H. X. Tang, On-chip strong coupling and efficient frequency conversion between telecom and visible optical modes, Physical Review Letters **117**, 123902 (2016).

[41] S. Ramelow, A. Farsi, Z. Vernon, S. Clemmen, X. Ji, J. Sipe, M. Liscidini, M. Lipson, and A. L. Gaeta, Strong nonlinear coupling in a Si_3N_4 ring resonator, Physical Review Letters **122**, 153906 (2019).
[42] Z.-Y. Wang, X. Xiong, J.-Y. Liu, Q. Gong, Y.-F. Xiao, and Q.-T. Cao, Strong-coupling dynamics of frequency conversion in an optical microresonator, Physical Review A **108**, 033521 (2023).
[43] C. Holmes and G. Milburn, Parametric self pulsing in a quantum opto-mechanical system, Fortschritte der Physik **57**, 1052 (2009).
[44] M. H. Seavey, Magnon-phonon interaction and determination of exchange constants in $CsMnF_3$, Physical Review Letters **23**, 132 (1969).
[45] V. I. Ozhogin, Indirect parallel pumping and biresonant frequency doubling in antiferromagnets, Soviet Journal of Experimental and Theoretical Physics **31**, 1121 (1970).
[46] B. Y. Kotyuzhanskii and L. A. Prozorova, Observation of a size effect produced as a result of parameteric excitation of spin waves in $FeBO_3$, Journal of Experimental and Theoretical Physics Letters **32**, 235 (1980).
[47] A. Sud, Y. Koike, S. Iihama, C. Zollitsch, S. Mizukami, and H. Kurebayashi, Parity-controlled spin-wave excitations in synthetic antiferromagnets, Applied Physics Letters **118** (2021).
[48] Y. Ashida, Z. Gong, and M. Ueda, Non-hermitian physics, Advances in Physics **69**, 249 (2020).
[49] V. Sokolov and V. Zelevinsky, Dynamics and statistics of unstable quantum states, Nuclear Physics A **504**, 562 (1989).
[50] H. Suhl, The theory of ferromagnetic resonance at high signal powers, Journal of Physics and Chemistry of Solids **1**, 209 (1957).
[51] L. Liu, T. Moriyama, D. C. Ralph, and R. A. Buhrman, Spin-torque ferromagnetic resonance induced by the spin hall effect, Physical Review Letters **106**, 036601 (2011).
[52] K. McNeil, P. Drummond, and D. Walls, Self pulsing in second harmonic generation, Optics Communications **27**, 292 (1978).
[53] P. Mandel and X.-G. Wu, Second-harmonic generation in a laser cavity, JOSA B **3**, 940 (1986).
[54] L. Lugiato, C. Oldano, C. Fabre, E. Giacobino, and R. Horowicz, Bistability, self-pulsing and chaos in optical parametric oscillators, Il Nuovo Cimento D **10**, 959 (1988).
[55] X.-G. Wu and P. Mandel, Intracavity second-harmonic generation with a periodic perturbation, JOSA B **2**, 1678 (1985).